An experimental and modeling study of ammonia with enriched oxygen content and ammonia/hydrogen laminar flame speed at elevated pressure and temperature

Krishna Prasad Shrestha[1], Charles Lhuillier[2,3], Amanda Alves Barbosa[2], Pierre Brequigny[2], Francesco Contino[3], Christine Mounaïm-Rousselle[2], Lars Seidel[4*], Fabian Mauss[1]

1. Thermodynamics and Thermal Process Engineering, Brandenburg University of Technology, Siemens-Halske-Ring 8, 03046 Cottbus, Germany
2. Univ. Orléans, INSA-CVL, PRISME, EA 4229, F45072, Orléans, France
3. Thermo and Fluid Dynamics (FLOW), Vrije Universiteit Brussel, Belgium
4. LOGE Deutschland GmbH, Burger Chaussee 25, 03044 Cottbus, Germany

***Corresponding author:** Lars Seidel, e-mail: Lars.Seidel@logesoft.com

Colloquium: Laminar flames

Word Count (Method 1):

Abstract	263
Main text	3409
References	700
Figure 1	224
Figure 2	178
Figure 3	225
Figure 4	138
Figure 5	182
Figure 6	305
Figure 7	177
Figure 8	133
Figure 9	356
Table 1	145
Total(excl. abstract)	6172

Color figures in the electronic version only.

Supporting information is available

Abstract

Laminar flame speeds of ammonia with oxygen-enriched air (oxygen content varying from 21-30 vol.%) and ammonia-hydrogen-air mixtures (fuel hydrogen content varying from 0-30 vol.%) at elevated pressure (1-10 bar) and temperature (298-473 K) were determined experimentally using a constant volume combustion chamber. Moreover, ammonia laminar flame speeds with helium as an inert were measured for the first time. Using these experimental data along with published ones, we have developed a newly compiled kinetic model for the prediction of the oxidation of ammonia and ammonia-hydrogen blends in freely propagating and burner stabilized premixed flames, as well as in shock tubes, rapid compression machines and a jet-stirred reactor. The reaction mechanism also considers the formation of nitrogen oxides, as well as the reduction of nitrogen oxides depending on the conditions of the surrounding gas phase. The experimental results from the present work and the literature are interpreted with the help of the kinetic model derived here. The experiments show that increasing the initial temperature, fuel hydrogen content, or oxidizer oxygen content causes the laminar flame speed to increase, while it decreases when increasing the initial pressure. The proposed kinetic model predicts the same trends than experiments and a good agreement is found with measurements for a wide range of conditions. The model suggests that under rich conditions the N_2H_2 formation path is favored compared to stoichiometric condition. The most important reactions under rich conditions are: $NH_2+NH=N_2H_2+H$, $NH_2+NH_2=N_2H_2+H_2$, $N_2H_2+H=NNH+H_2$ and $N_2H_2+M=NNH+H+M$. These reactions were also found to be among the most sensitive reactions for predicting the laminar flame speed for all the cases investigated.

Keywords: ammonia, laminar flame speed, kinetic modeling, ammonia-hydrogen, NO_x

1. Introduction

Ammonia is a carbon free energy carrier. Its technical application is slightly hindered by the comparable low laminar flame speed. To consider ammonia (NH_3) as single or blend fuel, it is essential to have a deep understanding of the detailed chemical processes of fuel oxidation to N_2 and H_2O and further oxidation to emission formation, mainly NO and NO_2. Moreover, the knowledge on NH_3 kinetics is also needed to improve the general NO_x formation model. Ammonia is the smallest nitrogen containing fuel molecule. Several NH_3-NO_x mechanisms have been developed in recent years, each with different conditions of interest [1–3]. Shrestha et al. [4] published their NH_3 model recently which covers a broad range of experimental conditions available from the literature, including NO_x formation and reduction in dependence on the surrounding environment. Mathieu et al. [1] established an ammonia oxidation mechanism, based on experiments in a Shock Tube (ST). They compared their work against nine different literature models to underline the large discrepancies between the ammonia mechanisms. Hayakawa et al. [5] measured laminar flame speeds of ammonia – air in a cylindrical combustion chamber under elevated pressure conditions. They compared their data against the prediction of five detailed mechanisms from the literature. Most mechanisms failed to predict laminar flame experiments.

Xiao et al. [6] performed a comparative study on the performance of 12 different NH_3-NO_x kinetic mechanisms to identify the best model. They used NH_3/H_2 laminar flame speed data from [7] and NH_3 ignition delay time data from [1] to rate the model predictions. The majority of the kinetic models could not reproduce the experimental data for the investigated range of equivalence ratios. Recently, Pochet et al. [8] and He et al. [9] studied autoignition of neat NH_3 and NH_3/H_2 blends in a rapid compression machine (RCM). Both studies assessed the performance of the various NH_3 kinetic models including our previous work [4] against their experimental data and concluded that

none of the mechanisms was able to reproduce the experiments satisfactorily. Han et al. [10] performed an experimental and kinetic modeling investigation on laminar flame speed for NH_3/air and different $NH_3/H_2/CO/CH_4$ air blends. The three investigated mechanisms from literature could not accurately predict the laminar burning velocity. Recently, Mei et al. [2] performed laminar flame speed experiments for oxygen enriched $NH_3/O_2/N_2$ blends. They modified our previous work [4] to reach an agreement with their experiments. Their selection of the base model was founded on a previous comparative study, including work from different groups.

In general, the discrepancies between the kinetic model predictions are expected as the experimental database for ammonia oxidation is not yet broad enough. Uncertainties are found in the rate kinetic data as well as in the thermochemistry. Further experimental data are needed to allow further improvement of the kinetic models. The conclusion above includes that the further oxidation of intermediates to NO_x is not yet fully understood. Several researchers have already put their effort into the development of an NH_3-NO_x kinetic model but still, a well-established and reliable model is not yet available. As discussed in [2] our recent model [4] was not validated for laminar flames but can be modified to include these experiments.

In this study, we present new experimental flame speed data together with a modification of our recent work to include these experiments in our validation database.

The aim of the present work is thus twofold:

1) to extend laminar flame speed data already published in [11], in the case of NH_3/H_2 blends at higher pressure than atmospheric one, and also in the case of neat NH_3 with enriched O_2 conditions. Moreover, additional NH_3 laminar flame speed measurement with He as an inert will be provided for the first time to investigate the influence of third body coefficients in pressure dependent reactions.

2) to improve our previous model [4], based on the improved and broadened experimental database.

This work is an ongoing effort to develop a reliable and comprehensive mechanism for NH_3 and NH_3/H_2 blends. Although the focus of this study is on laminar flame speed, the derived model is critically tested against the previous validation database; i.e. ignition delay times (IDT), speciation in jet-stirred reactors (JSR), and burner stabilized flames (BSF).

2. Experimental set-up and processing

The experiments were performed in the 4.2 L (inner diameter 200 mm) spherical stainless steel combustion chamber, fully described in [12,13]. The fresh gases are heated up to a maximum initial temperature of 473K by means of a heating wire. Before filling the sphere, a vacuum pump allows the evacuation of residual gases until a pressure <0.009 bar. Then all reactant gases are injected by a thermal flow meter. Before being introduced in the sphere, the inlet valve heats the mixture up to the required temperature with a maximum of 2 K uncertainty. To guarantee a perfectly homogeneous mixture, a fan runs during few seconds, but is stopped 10 s before the ignition to avoid any perturbation. The maximum deviation between the effective initial pressure inside the combustion chamber and the required initial pressure was estimated about 0.5%. Two tungsten electrodes (1 mm diameter) with a conventional capacitive discharge ignition system are used, with an ignition coil time charge of 3 ms (i.e. discharge energy of less than 100 mJ). The electrodes gap is adjusted to ensure a sufficient energy deposit to sustain the flame.

Experiments were carried out at various initial pressure, temperature, global equivalence ratio from 1-10 bar, 298-473 K and 0.8-1.4 respectively. The volume content of H_2, x_{H2}, was varied from 0 to 30% (in fuel). Synthetic air (20.9% O_2 /79.1% N_2) was used as ambient gas, but experiments were also performed for the neat ammonia cases with a variation of oxygen content, x_{O2} (23, 25,

27 and 30%vol, in oxidizer). Last, a set of experiments was also conducted by using He as inert gases for 27 and 30% vol. O_2 cases. For each condition, at least 3 tests were carried out in order to obtain average and standard deviation values, represented by error bars in the following figures.

To measure laminar flame speeds, the Schlieren technique was implemented thanks to two opposite and transparent windows (diameter 70mm). The Schlieren set-up is composed by a continuous LED, coupled with a 0.8 mm pinhole and 2 convex mirrors (864 mm focal length). At the focal point of the second mirror, a 0.5 mm dot is placed and two lenses (250 mm and 400 mm) allow to focus the Schlieren images on the Phantom v1210 high-speed CMOS ship. Images of 640 x 800 pixels² were recorded with a magnification ratio of 0.11 mm/pixel. The frame rate was adapted from 5 to 8kHz. The temporal evolution of the expanding spherical flame was then processed to get the flame front radius, r_f. The laminar flame propagation speed, V_s was calculated from the time derivative of r_f. The non-linear methodology as suggested by Kelley and Law [14] and Halter et al. [15] was used to estimate the unstretched laminar flame velocity V_s^0, as $\left(\frac{V_s}{V_s^0}\right)^2 \ln\left(\frac{V_s}{V_s^0}\right)^2 = -2\frac{L_b K}{V_s^0}$, with K the stretch rate impacting the flame, estimated by $K = \frac{2}{r_f}\frac{dr_f}{dt}$ and L_b the Markstein length for burned gases.

This methodology was applied for flame diameter greater than 6.5mm to avoid any ignition effect and lower than 25 mm corresponding to a burned gas volume less than 1.6% of sphere volume, to consider constant pressure chamber and avoid confinement effect.

Then the fundamental unstretched laminar burning velocity S_L^0 is obtained with the expansion factor, ρ_b/ρ_u as $S_L^0 = \frac{\rho_b}{\rho_u} V_s^0$, with ρ_b and ρ_u the burned and the unburned gases densities respectively.

For low unstretched laminar burning velocity (<20 $cm.s^{-1}$), radiative heat loss induced error can be of importance. Those effects were already addressed in [11]. In the present work, using the correlation of Yu et. al. [16], the worst case is obtained at 473 K, 3 bar where an underestimate of about 12% is calculated for neat ammonia corresponding to an absolute error of 1 cm/s. The error decreases down to 1% for the fastest flames.

3. Kinetic modeling

The kinetic model used in this work follows our previous publication [4] and was revised to predict the new experimental data determined in this work and in our recent work [11] for the wide range of conditions. In this work, the reaction rate parameter of several reactions was updated based on the literature study. The changes were made in the NH_3, NH_2, NH, N_2H_2, and H_2NO sub-mechanisms and modified reactions are listed in Table 1. The model developed in this work is validated against 104 sets (approximately 500 data points) of laminar flame speed data (covering ϕ = 0.7- 1.7, T = 298-473 K, P = 1-10 bar). The complete kinetic scheme is provided as supporting information (SI).

Table 1: List of reactions with updated rate parameter in the detailed model, found in the SI.

Reactions	**Source of adopted rate**
$NH_2+H(+M)=NH_3(+M)$	Altinay and Macdonald [17]
$NH_3+H=NH_2+H_2$	Nguyen and Stanton [18]
$NH_2+H=NH+H_2$	Samu et al. [19]
$NH_2+O=HNO+H$	Miller et al. [20] /2
$NH_2+HO_2=NH_3+O_2$	Sumathi et al. [21]
$NH_2+HO_2=H_2NO+OH$	Sumathi et al. [21]
$NH_2+HO_2=HNO+H_2O$	Sumathi et al. [21]
$NH_2+HO_2=HON+H_2O$	Sumathi et al. [21]
$N_2H_2+M=NNH+H+M$	Mei et al. [2] x 0.75
$N_2H_2+H=NNH+H_2$	Zheng et al. [22] x 2
$NH_2+NH=N_2H_2+H$	Klippenstein et al. [23] x 2
$NH_2+NH_2=N2H2+H_2$	Klippenstein et al. [23] x 2
NH+OH=HNO+H	Klippenstein et al. [23]
$NH+OH=N+H_2O$	Klippenstein et al. [23]

$H_2NO+O_2=HNO+HO_2$	Song et al. [3] x 0.78

4. Results and discussion

The symbols in figures are experimental data from this work or from the literature, lines are model prediction. All the simulations are performed with the LOGEresearch v1.10 [24] software suit. The model from this work is validated against 104 data sets of laminar flame speed measurements from different sources (32 data are from this work and 40 data (for NH_3/H_2) are from our recent work [11] and others are from published literature [2,5,7,10,11,25–32]).

4.1 Laminar flame speed of NH_3 and NH_3/H_2

Figure 1a displays the laminar flame speeds of NH_3/air at 1 atm and 298 K as a function of the equivalence ratio (ϕ). Literature data, own measurements and calculations are shown. Good agreement can be observed among the measured laminar flame speeds for fuel-lean and stoichiometric conditions while discrepancies can be observed on the fuel-rich side. The model (from this work) captures the experimental trends from lean to stoichiometric conditions very well. For lean and stoichiometric conditions, the model agrees with most measurements. For fuel-rich conditions, the best agreement is found with the older measurements from Ronney 1988 [31] and with the very recent experiments from Mei et al. 2019 [2]. Furthermore, particularly for fuel-rich conditions the model in this work shows an improved agreement against the measurements, compared to the model from our previous work [4]. This improvement is mainly due to the update in the rate parameters for the reactions involving N_2H_2 (listed in Table 1). Reaction flow analysis (see Fig. 2, only major paths are shown here) reveals that reaction paths involving N_2H_2 are favored more at rich conditions. As can be seen in Fig. 2 at rich environment (ϕ=1.4 – red numbers) most of the NH_2 reacts to N_2H_2 reacting with NH or self-recombining. This route increases its flux by

60% when compared to stoichiometric conditions. This increased importance of N_2H_2 formation via the NH_2 route is compensated by the shrink in the NH formation route.

Figure 1b shows the laminar flame speed of NH_3/H_2/air blends at stoichiometric and standard condition (1 atm, 298 K) at varying H_2 content (0-100%) in the fuel blend. Most measurements limit the hydrogen content to 60%. The measurements from Kumar et al. [32] at 60% H_2 and above diverge from other experimental measurements. It can be observed that the updated model from this work (solid line) accurately predicts the laminar flame speed. Calculations with our mechanism from prior work [4] is also shown (dashed line). It is found that for NH_3/H_2/air blends the reactions $NNH+O_2=N_2+HO_2$, $NH_2+O=HNO+H$ and $NH+OH=HNO+H$ are important for predicting laminar flame speed, with increasing importance with increasing H_2 content in the blend.

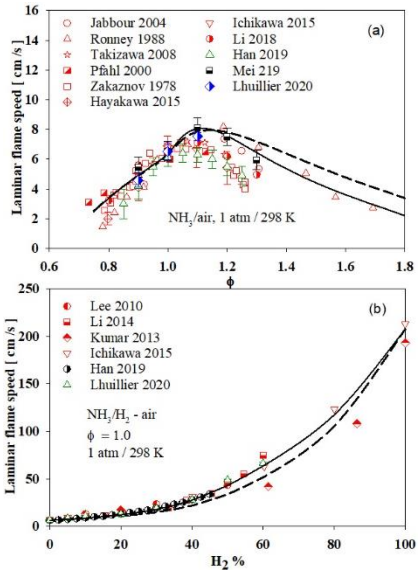

Figure 1: Laminar flame speed at 1 atm and 298 K for NH_3/air (a) and for stoichiometric conditions for NH_3/H_2/air (b). Symbols: measurements published literature [2,5,10,11,25,27–33]. Dashed lines: previous model [4], solid lines: this work.

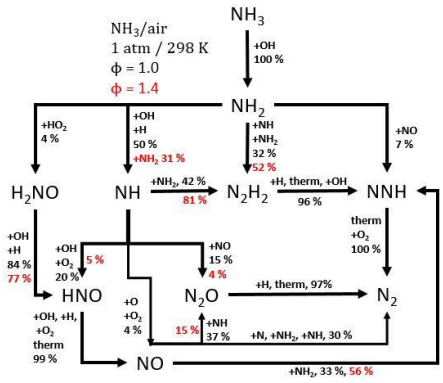

Figure 2: Integrated N-atom mass flux analysis at 1 atm and 298 K for ϕ = 1.0 and ϕ = 1.4 NH_3/air blends. Numbers are the percentage of the reactant forming the respective product. Major changes in flow highlighted by red for ϕ = 1.4.

Figure 3 shows measured laminar flames speeds (symbols) compared against the model predictions using our previous work [4] and the model improvements from this work for NH_3/H_2/air at 473 K and 1 bar [11] and 3 bar (present work). Simulations were performed using a detailed multicomponent diffusion model to consider the strong thermo diffusion of H and H_2. It can be seen that as the hydrogen content in the mixture is increased laminar flame speed is also increased. The experiments show peak laminar flame speed at ϕ = 1.1, which is well predicted by the models. It can be observed that below 10% H_2 the laminar flame speed does not increase significantly, but does for H_2 contents in the blend above 10% (see Fig. 1b). For 1 bar (Fig. 3a) at ϕ = 1.1 with 10% and 30% H_2, laminar flame speed is increased by factor 1.4 and 2.8 respectively and for 3 bar (Fig. 3b) at same conditions by factor 1.3 and 2.0 respectively compared to neat ammonia flame. This leads to the conclusion that the impact of H_2 on the laminar flame speed of NH_3/air is reduced with increasing pressure. Figure 3 also demonstrates that the model predictions from this work agree well with most measurements with a slight underestimation for 30% H_2 (Figure 3a) under lean to stoichiometric conditions.

Figure 4 shows new laminar flame speed data of NH_3/H_2/air at ϕ = 1.1, 473 K, and pressure of 5, 7 and 10 bar respectively as a function of H_2 content in the fuel blend. It can be observed that the model predicts slightly higher flame speeds compared to measurements but remain within the error margins of experiments. There are limited number of experimental data in literature at higher pressure (we believe this study is first to report data at 7 and 10 bar).

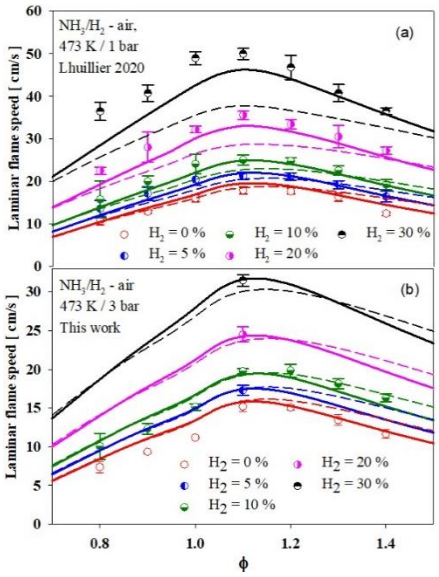

Figure 3: Laminar flame speeds of NH_3/H_2/air at 473 K and 1 bar (a) and 3 bar (b) at varying H_2 content. Symbols: measurements from [11] and this work. Dashed lines: previous model [4], solid lines: this work.

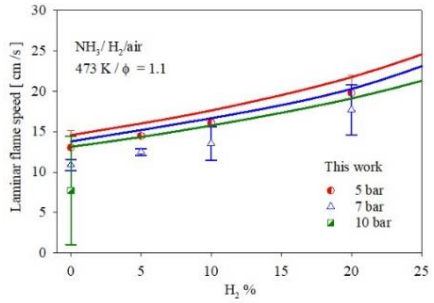

Figure 4: Laminar flame speed of NH_3/H_2/air at 473K and varying H_2 content at ϕ = 1.1 and 5-10 bar. Symbols: present measurements. Lines: simulations from this work.

To outline important reactions with regard to NH_3/H_2/air laminar flame speeds a reaction sensitivity analysis is conducted which is presented in Fig. 5 for ϕ = 1.0 at 1 bar and 473 K and different H_2 contents (0-30%) in the fuel blend. In Fig. 5 positive sensitivity means reaction promotes the reactivity (increased flame speed) and negative sensitivity means reaction retards the reactivity. The chain branching reaction from the hydrogen chemistry (O_2+H=OH+O) is also for ammonia the most sensitive reaction under all conditions. Its sensitivity increases as the H_2 content is increased and explains the accelerating laminar flame speed with increasing H_2 content. Other most sensitive reactions involve the NNH radical, which is a key radical in the ammonia oxidation chemistry. The thermal dissociation NNH=N_2+H competes with the oxidation NNH+O_2=N_2+HO_2. The former reaction promotes the reactivity by producing more reactive H-atoms while the latter retards the system reactivity by producing less reactive HO_2 radicals. Sensitivity increases with increasing H_2 content in the blend for both reactions. The reactions, NH_2+NO=NNH+OH and N_2H_2+M=NNH+H+M are chain branching reactions promoting the reactivity of the system. With respect to the increasing H_2 content, the sensitivity of the former reaction increases while sensitivity of later reaction decreases. A further important reaction is NH_2+NH=N_2H_2+H, with the highest contribution to the formation of N_2H_2 and consuming the important key radicals (NH_2 and NH). The sensitivity of this reaction also increases with increase in H_2 content. Similar observations can be drawn for other reactions as well. Additional model validation of NH_3/air and NH_3/H_2/air laminar flame speeds for wide range of experimental condition is shown in SI (see Fig. S1 – S8).

Furthermore, for comparison study simulation has also been performed using three different mechanisms from literature (Glarborg et al. [34], Otomo et al. [35] and Stagni et al. [36]). The

performance of these mechanisms against the experimental data (shown in Fig. 1, Fig. 3 and Fig. 4) are provided in SI (Fig. S12-S15). Among these, the model from Glarborg [34] overestimates the laminar flame speed at all conditions, Otomo's [35] underestimates mainly for NH_3/H_2 blends, and Stagni model [36] performance is similar as our mechanism from this work.

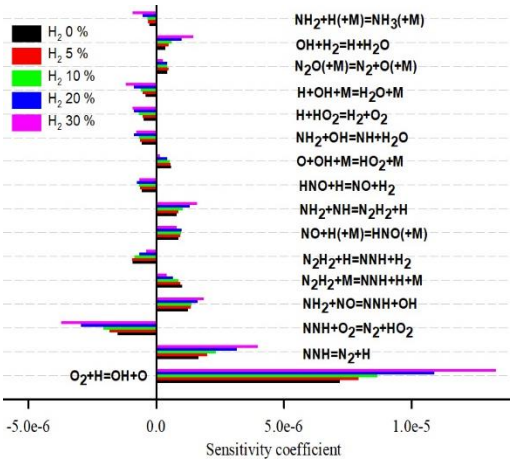

Figure 5: Reaction sensitivity analysis for laminar flame speed of NH_3/H_2/air at ϕ = 1.0, 1 bar and 473 K with varying H_2 content in the fuel blend.

4.2 Laminar flame speed of NH_3 with an enriched oxygen content

Figure 6 shows laminar flame-speed comparisons between model predictions and new measurements for $NH_3/O_2/N_2$ with varying O_2 content (21-30%) at 298 K (a), 323 K (b) and 373 K (c) as a function of ϕ. The experiments show that increasing the O_2 content increases the laminar flame speed and the same trend is predicted by the model. The sensitivity on O_2 is slightly overestimated, which is seen under lean conditions. The model follows the experimental trend very well for all the conditions. For completeness it is also stated that the agreement is better for 298 and 373 K than at 323 K. The laminar flame speed depends almost linearly on the O_2 content in the oxidizer (see also Fig. S17 in SI). The influence of O_2 is mainly explained by the increased adiabatic flame temperature. The influence of the chemistry is discussed in Fig. 7. It should be

noted that with increasing H_2 in fuel blend the growth is exponential while this does not hold true for O_2 (see Fig. 1b and Fig. S17).

To explore the important reactions for predicting the laminar flame speeds at varying O_2 content, reaction sensitivity analysis is performed. Figure 7 displays the 15 most sensitive reactions at ϕ = 1.0, 1 bar and 298 K. The highest sensitivity of the branching reaction $O_2+H=OH+O$ is expected. Its sensitivity increases with increasing O_2 content in the oxidizer. Most of the sensitive reactions are unchanged when compared to Fig. 5 (H_2 addition to the fuel). Reaction $NNH=N_2+H$ and $NNH+O_2=N_2+HO_2$ which showed an increased sensitivity trend with an increase in H_2 content in the NH_3/H_2/air blend (Fig. 5), shows a decreasing sensitivity trend with an increase in O_2 content. Similarly, reaction $N_2H_2+M=NNH+H+M$ and $N_2H_2+H=NNH+H_2$ show an increasing trend in sensitivity contrary to Fig. 5. However, other important reactions $NH_2+NO=NNH+OH$ and $NH_2+NH=N_2H_2+H$ show a similar trend decreasing and increasing. Hence the chemical effect of O_2 enrichment is more complex. It is, however governed by the chain branching reaction $O_2+H=OH+O$.

The prediction of different models from literature [34–36] was compared against the present experimental data (see SI Fig. S22 – Fig. S24). The model from Glarborg [34] overestimates the laminar flame speed at all conditions, Otomo's [35] underestimates mainly on the rich side, and Stagni model [36] performance is similar as our model from this work.

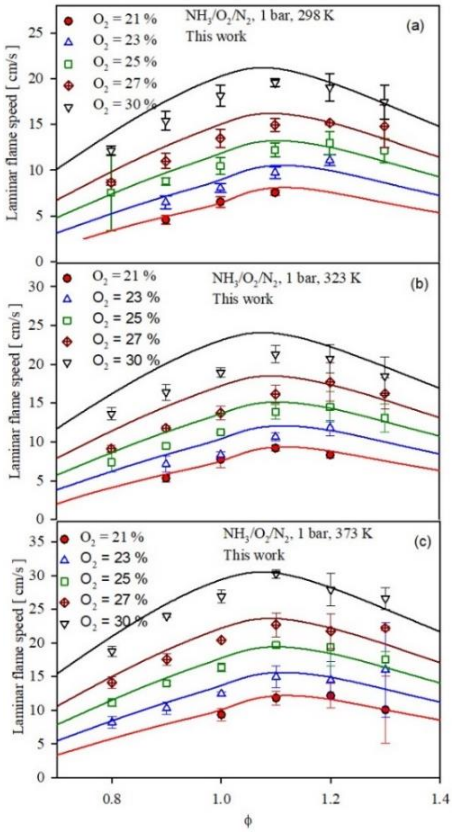

Figure 6: Laminar flame speed of $NH_3/O_2/N_2$ at 1 bar and different temperatures with varying O_2 content (21 – 30%). At 298 K (a), 323 K (b) and 373 K (c). Symbols: measurements from this work. Lines: model prediction from this work.

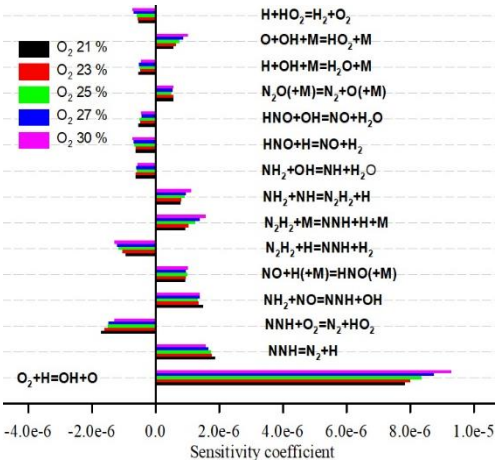

Figure 7: Reaction sensitivity analysis for laminar flame speed of $NH_3/O_2/N_2$ at $\phi = 1.0$, 1 bar and 298 K with varying O_2 content (21 – 30%).

Figure 8 shows the laminar flame speeds of NH_3/O_2/He blend compared to the model prediction for 27 and 30% O_2 at 373K and model predictions for 21% O_2. This experiment varies the heat capacity on the one hand, and the collision efficiency on the other hand of the inert gas in the oxidizer. The strong increase in laminar flame speed compared to experiments with N_2/O_2 oxidizer blends is mainly explained by the increased adiabatic flame temperature. The model predicts slightly higher laminar flame speed at lean and stoichiometric conditions and shows much better agreement on the rich side.

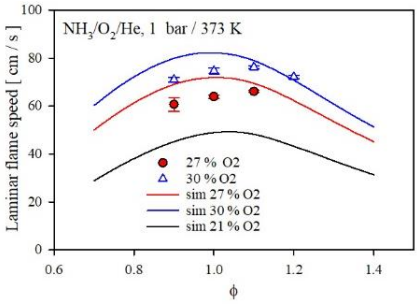

Figure 8: Laminar flame speed of NH_3/O_2/He at 1 bar and 373K and different O_2 contents. Symbols: measurements. Lines: simulation from this work.

4.3 Model validation against literature data for IDT, speciation in BSF and JSR

Finally, we demonstrate for completeness of this paper that the modified model still predicts the validation experiments from previous work. Figure 9a shows the comparison between the model predictions against selected experimental data for ignition delay times in shock tube [1] and RCM [9] for NH_3/O_2/Ar blend. The model predictions are in good agreement with the experimental data for a wide range of pressure over the whole temperature range investigated. Figure 9 (b: speciation in NH_3/NO/Ar, BSF (295K, 7.2kPa), (c, d): speciation during $H_2/O_2/N_2$ oxidation in JSR doped with 220 ppm of NO) compares the model prediction against the experimental data from the

literature and good agreement is found. Additional model validation for IDT, BSF, and JSR is shown in SI to offer a broad data base (Fig. S25 – S31).

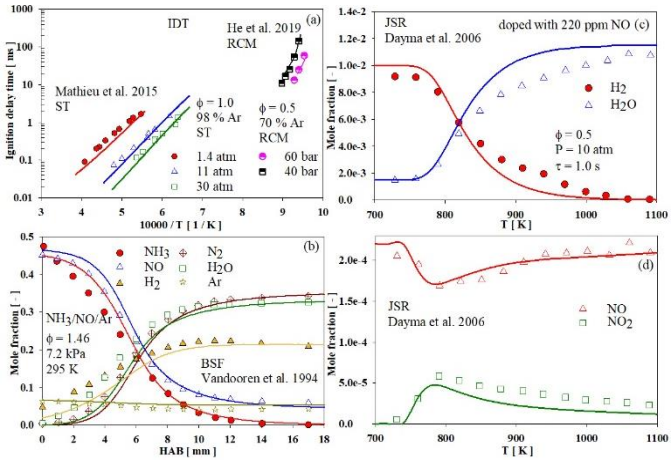

Figure 9: Comparison between model prediction and experimental data from literature for $NH_3/O_2/Ar$, IDT (in ST and RCM) (a); for $NH_3/NO/Ar$ (ϕ = 1.46), BSF (b); and for $H_2/O_2/NO$ (220 ppm)/N_2 (ϕ = 0.5, 10 atm, τ= 1.0 s), JSR (c, d). Symbols: measurements [1,37,38], lines: this work.

5. Conclusion

New laminar flame speed database of NH_3 in O_2-enriched air and NH_3/H_2 blends have been studied experimentally at 1-10 bar, 298-473 K using a constant pressure spherical combustion vessel. Based on the present measurements and published experimental data, a reaction mechanism for the oxidation of NH_3 and NH_3/H_2 blends is developed. A number of published experiments have been selected to demonstrate that important features of the ammonia chemistry are well captured by the mechanism that was modified to include laminar flame speed prediction. Overall, there is a good agreement between model predictions and experimental measurements for the wide range of experimental conditions investigated. It is found that laminar flame speed of neat ammonia can be

increased by increasing the oxygen content or using hydrogen as fuel blend. To rate the sensitivity of H_2 addition to the fuel blend or O_2 enrichment in the oxidizer we compared the data: for 30% H_2 (in fuel stream) or 30% O_2 (in oxidizer stream) the laminar flame speed of NH_3 is increased by factor 2.9 or 2.8 respectively. Hence, 9% increase of O_2 (compared to air) content has the same effect as 30% H_2 in the fuel blend.

Acknowledgements

The research leading to these results has received funding from the French Government's "Investissement d'Avenir" program: "Laboratoire d'Excellence CAPRYSSES" (Grant No ANR-11- LABX-0006-01).

References

[1] O. Mathieu, E.L. Petersen, Experimental and modeling study on the high-temperature oxidation of Ammonia and related NOx chemistry, Combust. Flame. 162 (2015) 554–570. doi:10.1016/j.combustflame.2014.08.022.

[2] B. Mei, X. Zhang, S. Ma, M. Cui, H. Guo, Z. Cao, Y. Li, Experimental and kinetic modeling investigation on the laminar flame propagation of ammonia under oxygen enrichment and elevated pressure conditions, Combust. Flame. 210 (2019) 236–246. doi:10.1016/j.combustflame.2019.08.033.

[3] Y. Song, H. Hashemi, J.M. Christensen, C. Zou, P. Marshall, P. Glarborg, Ammonia oxidation at high pressure and intermediate temperatures, Fuel. 181 (2016) 358–365. doi:10.1016/J.FUEL.2016.04.100.

[4] K.P. Shrestha, L. Seidel, T. Zeuch, F. Mauss, Detailed Kinetic Mechanism for the Oxidation of Ammonia Including the Formation and Reduction of Nitrogen Oxides, Energy & Fuels. 32 (2018) 10202−10217. doi:10.1021/acs.energyfuels.8b01056.

[5] A. Hayakawa, T. Goto, R. Mimoto, Y. Arakawa, T. Kudo, H. Kobayashi, Laminar burning velocity and Markstein length of ammonia/air premixed flames at various pressures, Fuel. 159 (2015) 98–106. doi:10.1016/j.fuel.2015.06.070.

[6] H. Xiao, A. Valera-Medina, Chemical Kinetic Mechanism Study on Premixed Combustion of Ammonia/Hydrogen Fuels for Gas Turbine Use, J. Eng. Gas Turbines Power. 139 (2017) 081504. doi:10.1115/1.4035911.

[7] J. Li, H. Huang, N. Kobayashi, Z. He, Y. Nagai, Study on using hydrogen and ammonia as fuels: Combustion characteristics and NOx formation, Int. J. Energy Res. 38 (2014) 1214–1223. doi:10.1002/er.3141.

[8] M. Pochet, V. Dias, B. Moreau, F. Foucher, H. Jeanmart, F. Contino, Experimental and numerical study, under LTC conditions, of ammonia ignition delay with and without hydrogen addition, Proc. Combust. Inst. 37 (2019) 621–629. doi:10.1016/J.PROCI.2018.05.138.

[9] X. He, B. Shu, D. Nascimento, K. Moshammer, M. Costa, R.X. Fernandes, Auto-ignition kinetics of ammonia and ammonia/hydrogen mixtures at intermediate temperatures and high pressures, Combust. Flame. 206 (2019) 189–200. doi:10.1016/j.combustflame.2019.04.050.

[10] X. Han, Z. Wang, M. Costa, Z. Sun, Y. He, K. Cen, Experimental and kinetic modeling study of laminar burning velocities of NH3/air, NH3/H2/air, NH3/CO/air and

NH3/CH4/air premixed flames, Combust. Flame. 206 (2019) 214–226. doi:10.1016/j.combustflame.2019.05.003.

[11] C. Lhuillier, P. Brequigny, N. Lamoureux, F. Contino, C. Mounaïm-Rousselle, Experimental investigation on laminar burning velocities of ammonia/hydrogen/air mixtures at elevated temperatures, Fuel. 263 (2020). doi:10.1016/j.fuel.2019.116653.

[12] P. Brequigny, G. Dayma, F. Halter, C. Mounaïm-Rousselle, T. Dubois, P. Dagaut, Laminar burning velocities of premixed nitromethane/air flames: An experimental and kinetic modeling study, Proc. Combust. Inst. 35 (2015) 703–710. doi:10.1016/j.proci.2014.06.126.

[13] B. Galmiche, F. Halter, F. Foucher, Effects of high pressure, high temperature and dilution on laminar burning velocities and Markstein lengths of iso-octane/air mixtures, Combust. Flame. 159 (2012) 3286–3299. doi:10.1016/j.combustflame.2012.06.008.

[14] A.P. Kelley, C.K. Law, Nonlinear effects in the extraction of laminar flame speeds from expanding spherical flames, Combust. Flame. 156 (2009) 1844–1851. doi:10.1016/j.combustflame.2009.04.004.

[15] F. Halter, T. Tahtouh, C. Mounaïm-Rousselle, Nonlinear effects of stretch on the flame front propagation, Combust. Flame. 157 (2010) 1825–1832. doi:10.1016/j.combustflame.2010.05.013.

[16] H. Yu, W. Han, J. Santner, X. Gou, C.H. Sohn, Y. Ju, Z. Chen, Radiation-induced uncertainty in laminar flame speed measured from propagating spherical flames, Combust. Flame. 161 (2014) 2815–2824. doi:10.1016/j.combustflame.2014.05.012.

[17] G. Altinay, R.G. Macdonald, Determination of the Rate Constants for the NH2(X2B1) + NH2(X2B1) and NH2(X2B1) + H Recombination Reactions in N2 as a Function of Temperature and Pressure, J. Phys. Chem. A. 119 (2015) 7593–7610. doi:10.1021/acs.jpca.5b00917.

[18] T.L. Nguyen, J.F. Stanton, Ab initio thermal rate coefficients for H + NH3 ⇌ H2 + NH2, Int. J. Chem. Kinet. 51 (2019) 321–328. doi:10.1002/kin.21255.

[19] V. Samu, T. Varga, I. Rahinov, S. Cheskis, T. Turányi, Determination of rate parameters based on NH2 concentration profiles measured in ammonia-doped methane–air flames, Fuel. 212 (2018) 679–683. doi:10.1016/J.FUEL.2017.10.019.

[20] J.A. Miller, M.D. Smooke, R.M. Green, R.J. Kee, Kinetic Modeling of the Oxidation of Ammonia in Flames, Combust. Sci. Technol. 34 (1983) 149–176. doi:10.1080/00102208308923691.

[21] R. Sumathi, S.D. Peyerimhoff, A quantum statistical analysis of the rate constant for the HO2 + NH2 reaction, Chem. Phys. Lett. 263 (1996) 742–748. doi:10.1016/S0009-2614(96)01283-3.

[22] J. Zheng, R.J. Rocha, M. Pelegrini, L.F.A. Ferrão, E.F.V. Carvalho, O. Roberto-Neto, F.B.C. MacHado, D.G. Truhlar, A product branching ratio controlled by vibrational adiabaticity and variational effects: Kinetics of the H + trans-N 2H 2 reactions, J. Chem. Phys. 136 (2012) 184310. doi:10.1063/1.4707734.

[23] S.J. Klippenstein, L.B. Harding, B. Ruscic, R. Sivaramakrishnan, N.K. Srinivasan, M. Su, J. V Michael, Thermal Decomposition of NH2 OH and Subsequent Reactions : Ab Initio Transition State Theory and Reflected Shock Tube Experiments, J. Phys. Chem. A. 113

(2009) 10241–10259. doi:10.1021/jp905454k.

[24] http://logesoft.com/loge-software/, (n.d.).

[25] K. Takizawa, A. Takahashi, K. Tokuhashi, S. Kondo, A. Sekiya, Burning velocity measurements of nitrogen-containing compounds, J. Hazard. Mater. 155 (2008) 144–152. doi:10.1016/j.jhazmat.2007.11.089.

[26] J.H. Lee, S.I. Lee, O.C. Kwon, Effects of ammonia substitution on hydrogen/air flame propagation and emissions, Int. J. Hydrogen Energy. 35 (2010) 11332–11341. doi:10.1016/j.ijhydene.2010.07.104.

[27] A. Ichikawa, A. Hayakawa, Y. Kitagawa, K.D. Kunkuma Amila Somarathne, T. Kudo, H. Kobayashi, Laminar burning velocity and Markstein length of ammonia/hydrogen/air premixed flames at elevated pressures, Int. J. Hydrogen Energy. 40 (2015) 9570–9578. doi:10.1016/j.ijhydene.2015.04.024.

[28] T. Jabbour, D.F. Clodic, Burning velocity and refrigerant flammability classification, ASHRAE Trans. 110 (2004) 522–533.

[29] V.F. Zakaznov, L.A. Kursheva, Z.I. Fedina, Determination of normal flame velocity and critical diameter of flame extinction in ammonia-air mixture, Combust. Explos. Shock Waves. 14 (1978) 710–713. doi:10.1007/BF00786097.

[30] U.J. Pfahl, M.C. Ross, J.E. Shepherd, K.O. Pasamehmetoglu, C. Unal, Flammability limits, ignition energy, and flame speeds in H2-CH4-NH3- N2O-O2-N2 mixtures, Combust. Flame. 123 (2000) 140–158. doi:10.1016/S0010-2180(00)00152-8.

[31] P.D. Ronney, Effect of Chemistry and Transport Properties on Near-Limit Flames at

Microgravity, Combust. Sci. Technol. 59 (1988) 123–141. doi:10.1080/00102208808947092.

[32] P. Kumar, T.R. Meyer, Experimental and modeling study of chemical-kinetics mechanisms for H 2-NH3-air mixtures in laminar premixed jet flames, Fuel. 108 (2013) 166–176. doi:10.1016/j.fuel.2012.06.103.

[33] Y. Li, M. Bi, B. Li, W. Gao, Explosion behaviors of ammonia–air mixtures, Combust. Sci. Technol. 190 (2018) 1804–1816. doi:10.1080/00102202.2018.1473859.

[34] P. Glarborg, J.A. Miller, B. Ruscic, S.J. Klippenstein, Modeling nitrogen chemistry in combustion, Prog. Energy Combust. Sci. 67 (2018) 31–68. doi:10.1016/j.pecs.2018.01.002.

[35] J. Otomo, M. Koshi, T. Mitsumori, H. Iwasaki, K. Yamada, Chemical kinetic modeling of ammonia oxidation with improved reaction mechanism for ammonia/air and ammonia/hydrogen/air combustion, Int. J. Hydrogen Energy. 43 (2018) 3004–3014. doi:10.1016/j.ijhydene.2017.12.066.

[36] A. Stagni, C. Cavallotti, S. Arunthanayothin, Y. Song, O. Herbinet, F. Battin-Leclerc, T. Faravelli, An experimental, theoretical and kinetic-modeling study of the gas-phase oxidation of ammonia, React. Chem. Eng. 5 (2020) 696–711. doi:10.1039/c9re00429g.

[37] J. Vandooren, J. Bian, P.J. Van Tiggelen, Comparison of experimental and calculated structures of an ammonianitric oxide flame. Importance of the NH2+ NO reaction, Combust. Flame. 98 (1994) 402–410. doi:10.1016/0010-2180(94)90178-3.

[38] G. Dayma, P. Dagaut, Effects of air contamination on the combustion of hydrogen-effect

of NO and NO2 addition on hydrogen ignition and oxidation kinetics, Combust. Sci. Technol. 178 (2006) 1999–2024. doi:10.1080/00102200600793171.

List of figure captions

Figure 1: Laminar flame speed at 1 atm and 298 K for NH_3/air (a) and for stoichiometric conditions for NH_3/H_2/air (b). Symbols: measurements published literature [2,5,32,33,10,11,25,27–31]. Dashed lines: previous model [4], solid lines: this work.

Figure 2: Laminar flame speeds of NH_3/H_2/air at 473 K and 1 bar (a) and 3 bar (b) at varying H_2 content. Symbols: measurements from [11] and this work. Dashed lines: previous model [4], solid lines: this work.

Figure 3: Laminar flame speeds of NH_3/H_2/air at 473 K and 1 bar (a) and 3 bar (b) at varying H_2 content. Symbols: measurements from [11] and this work. Dashed lines: previous model [4], solid lines: this work.

Figure 4: Laminar flame speed of NH_3/H_2/air at 473K and varying H_2 content at ϕ = 1.1 and 5-10 bar. Symbols: present measurements. Lines: simulations from this work.

Figure 5: Reaction sensitivity analysis for laminar flame speed of NH_3/H_2/air at ϕ = 1.0, 1 bar and 473 K with varying H_2 content in the fuel blend.

Figure 6: Laminar flame speed of $NH_3/O_2/N_2$ at 1 bar and different temperatures with varying O_2 content (21 – 30%). At 298 K (a), 323 K (b) and 373 K (c). Symbols: measurements from this work. Lines: model prediction from this work.

Figure 7: Reaction sensitivity analysis for laminar flame speed of $NH_3/O_2/N_2$ at ϕ = 1.0, 1 bar and 298 K with varying O_2 content (21 – 30%)

Figure 8: Laminar flame speed of NH_3/O_2/He at 1 bar and 373K and different O_2 contents. Symbols: measurements. Lines: simulation from this work.

Figure 9: Comparison between model prediction and experimental data from literature for NH_3/O_2/Ar, IDT (in ST and RCM) (a); for NH_3/NO/Ar (ϕ = 1.46), BSF (b); and for H_2/O_2/NO

(220 ppm)/N_2 (ϕ = 0.5, 10 atm, τ= 1.0 s), JSR (c, d). Symbols: measurements [1,37,38], lines: this work.

Supporting information

mech_Shrestha_et_al_38th_PROCI.txt – chemical kinetic mechanism

therm_Shrestha_et_al_38th_PROCI.txt – thermodata for species in the mechanism

trans_Shrestha_et_al_38th_PROCI.txt – transport data for species in the mechanism

Supporting_Information_Shrestha_et_al_38th_PROCI.pdf – additional mechanism validation figures and literature model comparison

Ammonia_Hydrogen_Flame_Speeds_Shrestha_et_al_38th_PROCI.xls - Laminar flame speed measured in this work

Supplemental Material - Mechanism (Reactions)

Supplemental Material - Mechanism (Thermodynamic Properties)

Supplemental Material - Mechanism (Transport properties)

Click here to access/download

Supplemental Material

trans_Shrestha_et_al_38th_PROCI_2020-5-8.txt